0090-9556/10/3802-323–331$20.00
DRUG METABOLISM AND DISPOSITION
Vol. 38, No. 2
29413/3555286
DMD 38:323–331, 2010
Printed in U.S.A.

Development of a Novel System for Estimating Human Intestinal Absorption Using Caco-2 Cells in the Absence of Esterase Activity

Kayoko Ohura, Hisae Sakamoto, Shin-ichi Ninomiya, and Teruko Imai

Graduate School of Pharmaceutical Sciences, Kumamoto University, Kumamoto, Japan (K.O., H.S., T.I.); and ADME & Tox. Research Institute, Sekisui Medical Co., Ltd., Ibaraki, Japan (S.N.)

Received July 9, 2009; accepted November 17, 2009

ABSTRACT:

Both mRNA and protein levels of the carboxylesterase (CES) isozymes, hCE1 and hCE2, in Caco-2 cells increase in a time-dependent manner, but hCE1 levels are always higher than those of hCE2. In human small intestine, however, the picture is reversed, with hCE2 being the predominant isozyme. Drugs hydrolyzed by hCE1 but not by hCE2 can be hydrolyzed in Caco-2 cells, but they are barely hydrolyzed in human small intestine. The results in Caco-2 cells can be misleading as a predictor of what will happen in human small intestine. In the present study, we proposed a novel method for predicting the absorption of prodrugs in the absence of CES-mediated hydrolysis in Caco-2 cells. The specific inhibition against CES was achieved using bis-*p*-nitrophenyl phosphate (BNPP). The optimal concentration of BNPP was determined at 200 μM by measuring the transport and hydrolysis of *O*-butyryl-propranolol (butyryl-PL) as a probe. BNPP concentrations of more than 200 μM inhibited 86% of hydrolysis of butyryl-PL, resulting in an increase in its apparent permeability. Treatment with 200 μM BNPP did not affect paracellular transport, passive diffusion, or carrier-mediated transport. Furthermore, the proposed evaluation system was tested for ethyl fexofenadine (ethyl-FXD), which is a superior substrate for hCE1 but a poor one for hCE2. CES-mediated hydrolysis of ethyl-FXD was 94% inhibited by 200 μM BNPP, and ethyl-FXD was passively transported as an intact prodrug. From the above observations, the novel evaluation system is effective for the prediction of human intestinal absorption of ester-type prodrugs.

The prediction of drug intestinal absorption is important for drug development and is currently evaluated primarily by measurement of in vitro cellular permeation using Caco-2 cell monolayers, a cell line derived from a human colon adenocarcinoma (Artursson et al., 2001). Confluent monolayers of Caco-2 cells spontaneously exhibit morphological and biochemical differentiation characteristics of mature enterocytes under standard culture conditions (Pinto et al., 1983). Caco-2 cells express several drug-metabolizing enzymes and transporters that are found in human enterocytes, including enzymes such as cytochrome P450, carboxylesterase (CES), and UDP-glucuronosyl transferase (UGT) (Sun et al., 2002; Borlak and Zwadlo, 2003; Siissalo et al., 2008), as well as uptake and efflux transporters such as human peptide transporter 1 (hPEPT1), organic anion-transporting polypeptide (OATP)-B (OATP2B1), P-glycoprotein (P-gp), breast cancer resistance protein (BCRP), and multidrug resistance-associated protein 2 (Hidalgo and Li, 1996; Tsuji and Tamai, 1996; Watkins, 1997). However, it has been reported that the expression levels of drug-metabolizing enzymes in Caco-2 cells are different from those in human small intestine. For example, the expression level of CYP3A4 in Caco-2 cells was shown to be considerably lower than that in human duodenal enterocytes and normal colorectal tissue (Raeissi et al., 1999; Nakamura et al., 2002), and human UGT1A10, an isozyme of the UGT 1A family, is expressed in extrahepatic tissues such as stomach, intestine, and colon, but only very low levels of expression were found in Caco-2 cells (Jeong et al., 2005).

We recently demonstrated that the expression of CES was significantly different in Caco-2 cells compared with that in human small intestine and/or colon tissue (Imai et al., 2005). CESs are the important esterases for the activation of prodrugs and are grouped in five subfamilies (CES1–CES5). The major CES isozyme in human small intestine is human CES2 isozyme (hCE2), whereas human CES1 isozyme (hCE1), is predominantly present in Caco-2 cells. The substrate specificities of hCE1 and hCE2 are different. The major intestinal CES, hCE2, hydrolyzes mainly the prodrug modified alcohol group of pharmacologically active drugs with a small acyl group. (Satoh et al., 2002; Imai, 2006). The few prodrugs grouped in this category are developed, such as CPT-11 and aspirin (Takai et al., 1997; Tang et al., 2006). In contrast, the prodrug modified carboxyl group of pharmacologically active drugs with a small alcohol group are preferentially hydrolyzed by hCE1 and have been developed as

Article, publication date, and citation information can be found at http://dmd.aspetjournals.org.
doi:10.1124/dmd.109.029413.

ABBREVIATIONS: CES, carboxylesterase; UGT, UDP glucuronosyltransferase; hPEPT1, human peptide transporter 1; OATP, organic anion-transporting polypeptide; P-gp, P-glycoprotein; BCRP, breast cancer resistance protein; hCE1, human carboxylesterase 1; hCE2, human carboxylesterase 2; CPT-11, irinotecan; BNPP, bis-*p*-nitrophenyl phosphate; PL, propranolol; FXD, fexofenadine; PMSF, phenylmethylsulfonyl fluoride; PNPB, *p*-nitrophenyl butyrate; HPLC, high-performance liquid chromatography; DMEM, Dulbecco's modified Eagle's medium; AP, apical; BL, basolateral; TEER, transepithelial electrical resistance; RT, reverse transcription; PCR, polymerase chain reaction; PBS, phosphate-buffered saline; BSA, bovine serum albumin; PVDF, polyvinylidene difluoride; PAGE, polyacrylamide gel electrophoresis; HBSS, Hanks' balanced salt solution; EBSS, Earle's balanced salt solution; MES, 2-(*N*-morpholino)ethanesulfonic acid.

pharmaceutical agents, for example, oseltamivir, meperidine, capecitabine, camostat mesylate, and angiotensin-converting enzyme inhibitors temocapril and enalapril (Takai et al., 1997; Satoh et al., 2002). These compounds recognized by hCE1 are hydrolyzed in Caco-2 cells but not in the small intestine. We have previously reported that temocapril is significantly converted to temocaprilat during transport across Caco-2 cell monolayers, because it is a good substrate for hCE1, despite not being hydrolyzed in human small intestine (Imai et al., 2005). The human intestinal absorption of temocapril may therefore be falsely estimated both in terms of absorption rate and absorbed molecular form. Because a number of prodrugs are grouped in hCE1 substrates, it is important to predict human small intestinal absorption of this type of drug in the early stage of drug screening. The establishment of Caco-2 cell monolayers without CES-mediated hydrolase activity would achieve this goal.

In the present study, we tried to develop a novel evaluation system by inhibiting CES activity in Caco-2 cell monolayers. We selected bis-*p*-nitrophenyl phosphate (BNPP) as an inhibitor for CES. BNPP can specifically inhibit CES but not other serine esterases (Block and Arndt, 1978; Mentlein et al., 1988). Because the inhibition of CES by BNPP is irreversible, the inhibition of CES-mediated hydrolysis can be continued for a long experimental period (Heymann and Krisch, 1967). First, the optimal treatment conditions for BNPP were confirmed by the measurement of hydrolysis and transport of *O*-butyryl-propranolol (butyryl-PL), a model prodrug, through Caco-2 cell monolayers. We then studied whether the treatment of Caco-2 cell monolayers with BNPP had any effect on carrier-mediated transport or paracellular and transcellular passive diffusion. Finally, we evaluated the permeability of ethyl-fexofenadine (ethyl-FXD), an ester derivative of FXD with ethanol, across Caco-2 cell monolayers under conditions of CES inhibition.

Materials and Methods

Materials. Human liver and small intestine microsomes were obtained from BD Gentest (Woburn, MA). No protease inhibitor such as phenylmethylsulfonyl fluoride (PMSF) was used during preparation of microsomes. Anti-hCE1 and anti-hCE2 antibodies were a kind gift from Dr. M. Hosokawa (Chiba Institute of Science, Chiba, Japan). Fast Red TR hemi(zinc chloride) salt, 3′3-diaminobenzidine, and *p*-nitrophenyl butyrate (PNPB) were purchased from Sigma-Aldrich (St. Louis, MO). BNPP, α-naphthylacetate, and *p*-nitrophenol were purchased from Nacalai Tesque (Kyoto, Japan). FXD and ethyl-FXD were synthesized according to the procedure of Di Giacomo et al. (1999). Butyryl-PL hydrochloride was synthesized from PL hydrochloride (Wako Pure Chemicals, Osaka, Japan) as described previously (Shameem et al., 1993). The identity and purity of these synthesized chemicals were confirmed by infrared, NMR, atomic analysis, and HPLC. [^{14}C]D-Mannitol (1.96 GBq/mmol) and [^{3}H]paclitaxel (1.52 GBq/mol) were purchased from Moravek Biochemicals, (Brea, CA). [^{3}H]Gly-Sar (2.22 GBq/mol) was obtained from American Radiolabeled Chemicals (St. Louis, MO). [^{3}H]Estrone-3-sulfate ammonium salt (1.70 GBq/mol) was obtained from PerkinElmer Life and Analytical Sciences (Waltham, MA). All other chemicals and reagents were of analytical grade.

Cell Culture. Caco-2 cells were purchased from American Type Culture Collection (Manassas, VA). Caco-2 cells (passages 30–40) were grown in 75-cm^2 culture flasks in a humidified incubator at 37°C under 5% CO_2 in air, in culture medium consisting of Dulbecco's modified Eagle's medium (DMEM) (Sigma-Aldrich) with 10% heat-inactivated fetal bovine serum, 0.1 mM nonessential amino acids, 2 mM L-glutamine, 100 U/ml penicillin, and 100 μg/ml streptomycin. Before reaching confluence, the cells were trypsinized with 0.25% trypsin and 0.53 mM EDTA and seeded at a density of 8.0×10^4 cells/cm^2 in culture medium on polycarbonate membranes (3-μm pore size, 24.5-mm diameter, Transwell 3414; Costar, Cambridge, MA). The culture medium [1.5 ml in the apical (AP) compartment and 2.6 ml in the basolateral (BL) compartment] was replaced every other day for the first week and daily thereafter. Transepithelial electrical resistance (TEER) was measured using a Millicell ERS ohmmeter (Millipore Corporation, Billerica, MA). Caco-2 cells were used for the transport experiments 21 to 28 days after seeding, when the TEER values exceeded 700 Ω · cm^2.

RNA Extraction and TaqMan Real-Time RT-PCR Analysis. Total RNA was extracted from the Caco-2 cell monolayers using an RNeasy Mini Kit and QIAshredder (QIAGEN, Hilden, Germany) following the manufacturer's instructions. TaqMan Real-Time RT-PCR was performed according to the procedure described previously (Nishimura et al., 2002). In brief, target mRNA was quantified by TaqMan Real-Time RT-PCR using an ABI PRISM 7700 Sequence Detection System (Applied Biosystems, Warrington, UK). β-Actin, hypoxanthine phosphoribosyltransferase 1, and peptidylprolyl isomerase A were selected as reference genes for normalization.

The sequences of the primers and probes were as follows: for hCE1, forward primer 5′-CCAGAGAGAGTCAACCCCTTCT-3′, reverse primer 5′-TCCTGCTTGTTAATTCCGACC-3′, and probe 5′-ATGCTGCT-GCTGAAAACACCTGAAGAGCTT-3′; and for hCE2, forward primer 5′-ACCGCAGTGGAGTCAGAGTTTC-3′, reverse primer 5′-ATGCT-GAGGTACAGGCAGTCCT-3′, and probe 5′-TTCAACATGACCT TCCCTTC-CGACTCC-3′. For reference genes, TaqMan Assay Reagents (Applied Biosystems) were used. Amplification and detection were performed with the following profile: 1 cycle at 48°C for 30 min, 1 cycle at 95°C of 10 min, and 50 cycles each at 95°C for 15 s and 60°C for 1 min. Reactions were carried out in triplicate.

Preparation of Caco-2 Cells 9000*g* Supernatant. Caco-2 cells cultured on Transwell were washed with ice-cold phosphate-buffered saline (PBS) and then detached with a spatula. The harvested cells were suspended in ice-cold SET buffer (292 mM sucrose, 1 mM EDTA, and 50 mM Tris) and then homogenized using a Polytron homogenizer (Polytron-Aggregate; Kinematica, Littau, Switzerland) and Potter-Elvehjem Teflon-glass homogenizer under ice-cold conditions. The homogenates were centrifuged at 9000*g* for 20 min at 4°C to obtain the supernatant (S9) fraction. Protein contents were determined with bovine serum albumin (BSA) as the standard (Bradford, 1976). These preparations were stored at −80°C until use.

Western Blot Analysis. Caco-2 cell S9 (for the detection of hCE1, 0.8 μg; for the detection of hCE2, 30 μg) were separated on a 7.5% SDS-polyacrylamide gel and transferred electrophoretically to a polyvinylidene difluoride (PVDF) membrane (Immobilon-P; Millipore Corporation). After blocking in PBS with 0.05% Tween 20 and 3% BSA, the PVDF membrane was probed with anti-hCE1 antibody or anti-hCE2 antibody diluted 1:1000 in PBS with 0.05% Tween 20 (TPBS). After subsequent washes with PBS, membranes were incubated with peroxidase-conjugated AffiniPure goat anti-rabbit IgG (Jackson ImmunoResearch Laboratories, Suffolk, UK) diluted 1:5000 in TPBS. The immunoreactivity was revealed by adding 3′3-diaminobenzidine and hydrogen peroxide in 50 mM Tris-HCl buffer (pH 7.6).

Staining for Esterase Activity. Staining for esterase activity after nondenaturing polyacrylamide gel electrophoresis (PAGE) was performed as described previously (Imai et al., 2005). In brief, 5 μg of human liver or small intestine microsomal protein and 25 μg of Caco-2 cell S9 protein were loaded per lane. After electrophoresis, the bands containing esterase were stained by complex formulation between Fast Red TR hemi(zinc chloride) salt, a dyeing agent, and α-naphthol produced by hydrolysis of α-naphthylacetate, a substrate of esterase.

Treatment of Caco-2 Cell Monolayers with BNPP. Caco-2 cell monolayers were gently washed twice with Hanks' balanced salt solution (HBSS), containing 1.3 mM $CaCl_2$, 0.81 mM $MgSO_4$, 5.4 mM KCl, 0.44 mM KH_2PO_4, 137 mM NaCl, 0.34 mM Na_2HPO_4, 4.4 mM $NaHCO_3$, 25 mM D-glucose, 11 mM HEPES, and 6 mM NaOH, pH 7.4, followed by preincubation of both the AP and BL sides with 0, 100, 200, 300, or 500 μM BNPP dissolved in HBSS (pH 7.4) for 40 min at 37°C. The monolayers were then washed three times with DMEM, followed by preincubation of both AP and BL sides with fresh DMEM for 40 min at 37°C to completely remove BNPP nonspecifically bound to Caco-2 cell monolayers. The cell monolayers were washed again with fresh DMEM and then used for the transport experiments.

Transport Experiments. The Caco-2 cell monolayers treated with BNPP or sham-treated with HBSS were equilibrated with transport buffer for 10 min. Each chemical solution was then added to either the AP (1.5 ml) or BL (2.6 ml) side, and samples were sequentially taken from the donor and receiver compartments. The volume removed from the receiver side was always replaced with fresh transport buffer. All subsequent procedures were performed at 37°C.

The integrity of cell monolayers was checked by measuring TEER and trypan blue staining.

The following solutions were used as transport buffers. For transport experiments of butyryl-PL and PL, Earle's balanced salt solution (EBSS) containing 2.4 mM $CaCl_2$, 0.81 mM $MgSO_4$, 5.4 mM KCl, 116 mM NaCl, 1 mM NaH_2PO_4, 26 mM $NaHCO_3$, 25 mM D-glucose, and 9.1 mM MES, pH 6.0, without BSA and HBSS (pH 7.4) with 3% BSA were used on the AP and BL sides, respectively. The half-lives for hydrolysis of butyryl-PL in buffer were 80.2 and 12.4 h in the AP and BL sides, respectively. For transport of ethyl-FXD, FXD, [^{14}C]D-mannitol, and [^{3}H]paclitaxel, HBSS (pH 7.4) was used on both sides. For [^{3}H]Gly-Sar, HBSS (pH 7.4) or EBSS (pH 6.0) was used in the AP compartment and HBSS (pH 7.4) was used in the BL compartment. For [^{3}H]estrone-3-sulfate, EBSS (pH 6.0) and HBSS (pH 7.4) were used in the AP and BL compartments, respectively.

For measurement of sample concentrations of [^{14}C]D-mannitol, [^{3}H]Gly-Sar, [^{3}H]paclitaxel, and [^{3}H]estrone-3-sulfate, radioactivity was immediately counted in 2 ml of aqueous counting scintillant (GE Healthcare, Little Chalfont, Buckinghamshire, UK) by a liquid scintillation counting (Beckman LS 6500; GMI, Albertville, MN). The samples from other substrates were assayed by HPLC. Sample preparation for analysis by HPLC was as follows. For ethyl-FXD and FXD, the samples were mixed with an equal volume of organic solvent consisting of acetonitrile-methanol (2:1, v/v). After centrifugation of the mixture at 1600*g* for 10 min, the supernatant (50 μl) was injected onto the HPLC column. For butyryl-PL and PL, the samples were mixed with phosphoric acid (final concentration 21 mM) and equal volumes of acetonitrile. After centrifugation of the mixture at 1600*g* for 30 min, the supernatant (100 μl) was injected.

For measurement of cellular concentrations, Caco-2 cell monolayers were washed twice with HBSS after the transport experiment, and the cells were harvested and weighed. One milliliter of methanol was added to the cells, followed by sonication and vortexing. The cell mixtures were centrifuged at 1600*g* for 10 min, and the supernatants were evaporated. The residue was redissolved in the HPLC mobile phase and injected onto the HPLC column. The protein contents per well of Caco-2 cell monolayer were calculated from the protein content per Caco-2 cell weight. The cellular accumulation was represented as a drug amount per milligram of protein per hour of transport time. The apparent permeability coefficients, P_{app} (centimeters per second), were calculated using the following equation: $P_{app} = dQ/dt/A/C_0$, where dQ/dt is the rate of appearance of drug in the receiver compartment (steady-state flux, micromoles per second), A is the surface area of the monolayer (4.71 cm^2), and C_0 is the initial drug concentration (micromolar) in the donor compartment.

Hydrolysis Experiments. Hydrolysis experiments were performed on ester derivatives using human small intestine microsomes and Caco-2 cell S9. Caco-2 cell S9 used for the hydrolysis experiments was prepared as follows. Cell monolayers treated with 200 μM BNPP or sham-treated with HBSS were equilibrated and incubated with HBSS for 2 h at 37°C. The cell monolayers were washed twice with HBSS to completely remove free BNPP, and S9 was prepared.

Microsomes or S9 were diluted with HEPES buffer (50 mM, pH 7.4) at an appropriate protein concentration. After preincubation of the microsomes or S9 solution for 5 min at 37°C, the reaction was started by adding the substrate dissolved in dimethyl sulfoxide. The final concentration of dimethyl sulfoxide in the hydrolyzing incubation samples was maintained at 0.5%, which had no effect on hydrolase activity.

For the hydrolysis of butyryl-PL, the reaction was terminated by adding 5 ml of ethyl acetate and 0.5 ml of saturated NaCl solution adjusted to pH 4.0 with phosphoric acid. After the samples had been shaken for 10 min, the isolated ethyl acetate was evaporated, and the residue was redissolved in HPLC mobile phase and injected onto an HPLC column.

For the hydrolysis of PNPB, the reaction was initiated by the addition of PNPB (final concentration: 500 μM). Then the formation of *p*-nitrophenol was spectrophotometrically determined by the initial linear increase in absorbance at 405 nm (V-530; Jasco, Tokyo, Japan).

For the hydrolysis of ethyl-FXD, the reaction was terminated by adding an equal volume of ice-cold organic solvent consisting of acetonitrile-methanol (2:1, v/v). After centrifugation of the reaction mixture at 1600*g* for 10 min, the supernatant was injected onto the HPLC column.

HPLC Analysis. The HPLC system comprised a PU-980 pump, an AS-950 autosampler, a UV-2075 Plus detector, an FP-1520S fluorescence detector, and a CO-965 column oven (Jasco) and a Chromatopac C-R7A Plus data application apparatus (Shimadzu, Kyoto, Japan). For determination of FXD and ethyl-FXD, a Wakosil-II 5C8 HG column (5 μm, 4.6 $\times$ 150 mm i.d.; Wako Pure Chemicals) was used with a mobile phase of acetonitrile-methanol-12 mM ammonium acetate (pH 4.0, 39:10:51, v/v/v) at a flow rate of 1.0 ml/min. FXD and ethyl-FXD were detected at a wavelengths of 218 nm. For determination of the PL enantiomer, a CHIRALCEL OD column (10 μm, 4.6 $\times$ 250 mm i.d.; Daicel Chemical Industries, Ltd., Tokyo, Japan) was used with a mobile phase of hexane-ethanol-diethylamine (90:10:1.0, v/v/v) at a flow rate of 1.0 ml/min. For determination of racemic PL and butyryl-PL in the transport experiment, a LiChrosorb RP-select B column (7 μm, 4 $\times$ 250 mm i.d.; Merck, Darmstadt, Germany) was used with a mobile phase of acetonitrile-20 mM potassium dihydrogen phosphate (50:50, v/v) at a flow rate of 1.0 ml/min. PL and butyryl-PL were detected at excitation and emission wavelengths of 285 and 340 nm, respectively. The temperature of the column was maintained at 40°C. All substrates and hydrolysates were clearly separated and were measured in a quantitatively linear range.

Results

Time Course of Expression Levels of hCE1 and hCE2 in Caco-2 Cells Cultured on Transwell. The expression levels of hCE1 and hCE2 were periodically evaluated in Caco-2 cells cultured on Transwell. As shown in Fig. 1a, TaqMan Real-Time RT-PCR showed the time-dependent increase of hCE1 and hCE2 mRNA. However, the expression level of hCE2 mRNA was always lower than that for hCE1 mRNA during the culture period. hCE2 mRNA slowly increased before reaching a plateau at 3 weeks, whereas hCE1 mRNA increased linearly for 4 weeks after seeding. Similar results were obtained in the case of normalization by other genes, hypoxanthine phosphoribosyltransferase 1 and peptidylprolyl isomerase A (data not shown). In accordance with their mRNA levels, the protein levels of hCE1 and hCE2 also increased in a time-dependent manner as evaluated by Western blot analysis (Fig. 1b). Furthermore, as shown in Fig. 1c, the staining intensity of esterase bands in nondenaturing PAGE was time dependently increased. The expression pattern of esterases in Caco-2 cell cultured for long period was very similar to that in the human liver. These results agree with our previous data on the expression of esterase in Caco-2 cells grown in culture flasks for a week (Imai et al., 2005).

Transport and Hydrolysis of Butyryl-PL in Caco-2 Cell Monolayers. The transport and hydrolysis of butyryl-PL, which is a good substrate for CES, were examined in Caco-2 cell monolayers. Figure 2 shows the AP-to-BL transport of butyryl-PL across the Caco-2 cell monolayers. Butyryl-PL levels rapidly decreased on the AP side, indicating its rapid incorporation into the cells (Fig. 2a). However, PL was mainly transported into the BL side in comparison with butyryl-PL. Butyryl-PL was favorably hydrolyzed during transport across Caco-2 cell monolayers, and the intracellularly produced PL was effluxed from the cells into both AP and BL sides. The amount of PL from Caco-2 cells transported to the AP compartment (pH 6.0) was much larger than that into the BL compartment (pH 7.4). In this experiment, the AP side was adjusted to pH 6.0, and pH 7.4 HBSS containing 3% BSA was used as a buffer on the BL side to prevent the chemical hydrolysis of butyryl-PL. PL is a typical compound that permeates by passive diffusion according to the pH partition hypothesis. Therefore, intracellularly produced PL was preferentially transported from the cells into the AP compartment (pH 6.0) rather than the BL compartment (pH 7.4), because of its weak basicity (pK_a 9.44). The pH-dependent transport of PL across Caco-2 cell monolayers has been reported previously (Yamashita et al., 1997; Masaki et al., 2006). The total amount of PL transported to both

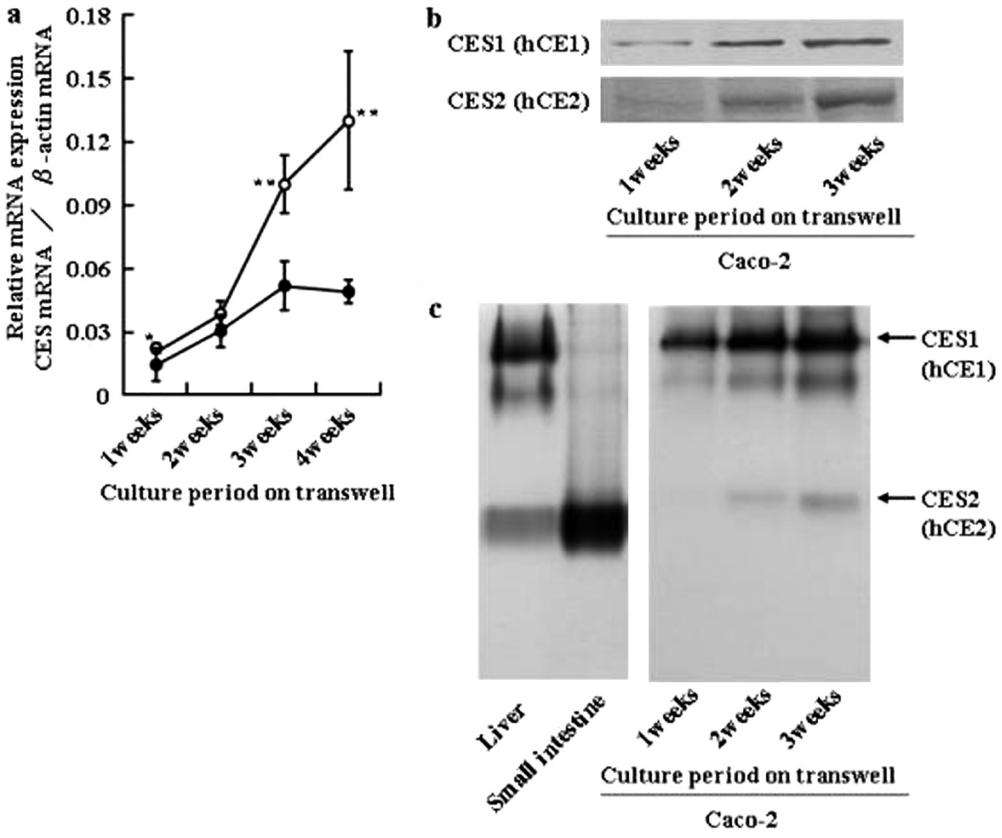

FIG. 1. Time profile of mRNA and protein expression levels of hCE1 and hCE2 in Caco-2 cells cultured on Transwell. a, relative gene expression levels normalized to β-actin by TaqMan Real-Time RT-PCR. ○, hCE1 expression; ●, hCE2 expression. Each point shows the mean ± S.D. of triplicate analyses. Statistical differences were determined by unpaired t test. After 2 weeks of culture all levels are significantly greater than after a 1-week culture period. **, $p < 0.01$; *, $p < 0.05$, both in comparison with hCE2. b, Western blot analysis using anti-hCE1 and anti-hCE2 antibodies. For the detection of hCE1 and hCE2, 0.8 and 30 μg of Caco-2 cell S9 proteins were subjected to SDS-PAGE and transferred electrophoretically to PVDF membrane for immunostaining. c, esterase activity staining after nondenaturing PAGE using α-naphthylacetate. The quantities of tissue microsomes and Caco-2 cell S9 proteins loaded in lanes were 5 and 25 μg, respectively. Arrows indicate bands corresponding to each CES isozyme.

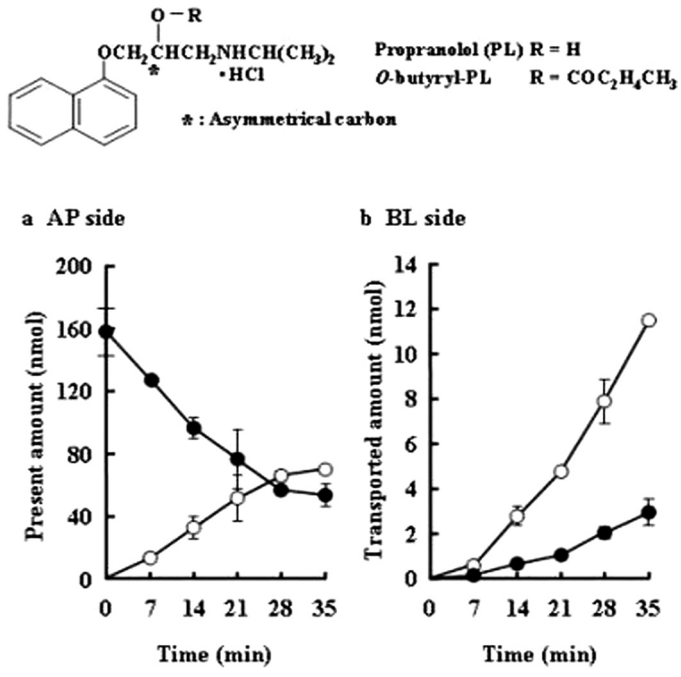

FIG. 2. Structure of butyryl-PL and the AP-to-BL transport of butyryl-PL (100 μM) across Caco-2 cell monolayers. a, the present amount of butyryl-PL and PL in AP side (pH 6.0, EBSS buffer). b, transported drugs in BL side (pH 7.4, HBSS buffer with 3% BSA). ●, butyryl-PL; ○, PL. Each point represents the mean ± S.D. (n = 3).

sides after 35 min (79.7 ± 2.49 nmol) was approximately half of the initial amount of butyryl-PL (158 ± 15.3 nmol) applied, indicating that butyryl-PL is sequentially hydrolyzed by esterase after incorporation into Caco-2 cells. These results suggest that butyryl-PL is a good marker compound for determining the treatment condition of Caco-2 cell monolayers with BNPP.

Determination of Treatment Conditions of Caco-2 Cell Monolayers with BNPP. First, the transport of BNPP across the Caco-2 cell monolayers was examined to determine the optimal length of the treatment period with BNPP. BNPP could be detected in the receiver compartment 10 min after 200 μM BNPP was applied on the AP side. The amount of transported BNPP increased linearly with the passage of time, and the intracellular concentration of BNPP reached a steady state at 40 min (data not shown). Therefore, it was decided that Caco-2 cell monolayers should be treated with BNPP in both AP and BL sides for 40 min to obtain complete inhibition of CES.

Second, the optimal BNPP concentration was determined. After treatment of Caco-2 cell monolayers with 0 to 500 μM BNPP for 40 min, BNPP was thoroughly washed out of both sides by incubation with DMEM for 40 min and equilibration with HBSS for 10 min. Butyryl-PL was then applied to the AP side of Caco-2 cell monolayers. The P_{app} and percentage of hydrolysis of butyryl-PL across the Caco-2 cell monolayers were determined (Table 1). The P_{app} value of butyryl-PL itself increased approximately three times after treatment with 100 μM BNPP and was constant up to 500 μM BNPP. The coefficients of variation of P_{app} values ranged from 2 to 11%, but there was no statistically significant difference in the range of 100 to 500 μM BNPP. The percentage of hydrolysis was calculated from the ratio between the initial applied amount of butyryl-PL and the total amount of PL in both AP and BL sides after 35 min; it was decreased by treatment with BNPP. The maximal effect of BNPP was achieved at 200 μM, and no significant difference in the percentage of hydrolysis on treatment with 200 to 500 μM BNPP was observed. Furthermore, treatment with 0 to 500 μM BNPP did not cause any significant change in the TEER or membrane cytotoxicity as visualized by trypan

TABLE 1

P_{app} and the percentage of hydrolysis for the transport of butyryl-PL through Caco-2 cell monolayers treated with BNPP

Values represent the mean ± S.D. (n = 3).

BNPP Conc.	P_{app}	CV	Percentage of Hydrolysis
	$\times 10^{-7}$ cm/s	%	%
0 μM	34.6 ± 8.20**	23.7	50.6 ± 3.31**
100 μM	115 ± 10.5	9.11	13.2 ± 2.32*
200 μM	118 ± 7.82	6.65	7.32 ± 0.513
300 μM	110 ± 2.62	2.40	7.24 ± 0.312
500 μM	122 ± 13.8	11.4	7.51 ± 0.897

CV, coefficient of variation of Papp values.
* $p < 0.05$, indicates statistically significant differences compared with 200 μM BNPP.
** $p < 0.01$.

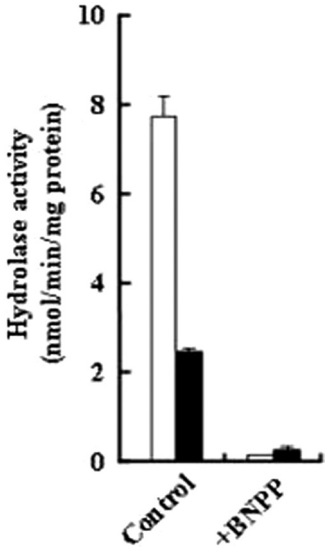

FIG. 3. Hydrolysis of butyryl-PL (100 μM) in Caco-2 cell S9 prepared from cell monolayers, untreated or treated with 200 μM BNPP as described in the procedure for the transport experiments. Caco-2 cell S9 was diluted with 50 mM HEPES buffer (pH 7.4) at 100 μg/ml. □, hydrolase activity for *R*-butyryl-PL; ■, hydrolase activity for *S*-butyryl-PL. Each column represents the mean ± S.D. (n = 3).

blue (data not shown). Consequently, the optimal treatment concentration of BNPP was determined to be 200 μM.

In the present study, BNPP treatment did not achieve complete inhibition of butyryl-PL hydrolysis during transport across Caco-2 cell monolayers. The comparison of percentage hydrolysis between the control (0 μM BNPP) and inhibited condition (200 μM BNPP) suggests that approximately 86% of hydrolase activity in Caco-2 cells is inhibited. Therefore, we examined whether CESs were incompletely inhibited by treatment with BNPP at 200 μM or above. After treatment with 0 and 200 μM BNPP, the cell monolayers were incubated with HBSS for 2 h; and then their cellular S9 fraction was prepared. As shown in Fig. 3, *R*-butyryl-PL was preferentially hydrolyzed by hCE1 in the control cell S9 (*R*/*S* ratio 3.0), whereas in the BNPP-treated cell S9, the hydrolysis rate of the *R*- and *S*-isomers was nearly identical and the hCE1-specific hydrolysis for *R*-butyryl-PL was 98% inhibited. These results indicate that BNPP is able to almost completely inhibit specific hydrolysis by CES. However, the activities of dipeptidyl peptidase-IV and aminopeptidase in Caco-2 cell S9 were not inhibited at all by BNPP (data not shown). These data suggest that the activity remaining after treatment with more than 200 μM BNPP might be attributed to other esterases present in the cellular membrane.

Effect of BNPP on Drug Transport via Paracellular and Transcellular Routes across Caco-2 Cell Monolayers. In general, drugs are transported across Caco-2 cell monolayers by various pathways, such as paracellular transport, transcellular passive diffusion, and carrier-mediated transport. The effect of BNPP on membrane permeability was evaluated using specific marker compounds for the respective permeation pathways. D-Mannitol and PL were selected as markers for passive diffusion of paracellular and transcellular routes, respectively. Gly-Sar, paclitaxel, and estrone-3-sulfate were selected as markers for carrier-mediated transport.

Figure 4 shows the P_{app} values for the transport of each compound across Caco-2 cell monolayers with or without treatment with 200 μM BNPP. The rather small P_{app} of [^{14}C]D-mannitol was nearly the same both with and without BNPP. The pH-dependent passive diffusion of PL, which is responsible for transport to the AP compartment (pH 6.0) rather than the BL compartment (pH 7.4), was not affected by treatment with BNPP. The results for D-mannitol and PL indicate no effect of BNPP on passive diffusion in Caco-2 cell monolayers. Furthermore, H^+-coupled uptake of [^{3}H]Gly-Sar by hPEPT1, which is functionally accelerated under the weakly acidic conditions of the AP side (pH 6.0), was not affected by treatment with BNPP. No statistical differences between control and treatment with 200 μM BNPP on the efflux transport of [^{3}H]paclitaxel via P-gp on the brush-border membrane was observed. Furthermore, the treatment with BNPP did not affect the transport of [^{3}H]estrone-3-sulfate, which is a substrate for OATP2B1, sodium-dependent organic anion transporter, and BCRP in AP membrane and also is a substrate for organic solute transporter α/β in BL membrane (Gram et al., 2009). These results suggest that BNPP has minimal influence, if any, on carrier-mediated transport.

Evaluation of the Transport of Ethyl-FXD through Caco-2 Cell Monolayers after Treatment with BNPP. As shown in Fig. 5, Ethyl-FXD, an ethyl ester of FXD, was barely hydrolyzed in human small intestine microsomes, although PNPB, a marker for human intestinal hydrolysis, was rapidly hydrolyzed. However, Caco-2 cell S9 showed high hydrolase activity for ethyl-FXD and low activity for PNPB. These results make it difficult to predict the human intestinal absorption of ethyl-FXD using Caco-2 cell monolayers. However, treatment of the cells with 200 μM BNPP prevented the hydrolysis of ethyl-FXD, allowing us to evaluate the AP-to-BL transport of ethyl-FXD through the Caco-2 cell monolayers in the presence or absence of inhibition of CES activity by BNPP (Fig. 6).

In control Caco-2 cell monolayers without BNPP, ethyl-FXD rapidly disappeared from the AP compartment and was taken up into the Caco-2 cells, where it accumulated at high concentrations because of its hydrophobicity and basicity. Subsequently, ethyl-FXD was slowly transported to the BL side, whereas FXD, an intracellularly hydrolyzed product, was transported into both AP and BL sides. The amount of FXD transported to the receiver compartment was three times that of ethyl-FXD within 2 h. The concentration of FXD in the AP compartment during transport was always higher than that in the BL compartment. The transport of FXD itself was examined in the presence of 200 μM BNPP. As shown in Table 2, the P_{app} value for the AP-to-BL transport of FXD was close to that for D-mannitol (Fig. 4a), whereas BL-to-AP transport of FXD was approximately three times higher. These results confirm the previous report of Perloff et al. (2002). It is suggested that FXD has a low membrane permeability and efflux via transporters such as P-gp and that FXD produced in Caco-2 cells is preferentially excreted into the AP side rather than the BL side.

In the transport experiment across Caco-2 cell monolayers after treatment with BNPP, the marked decrease of ethyl-FXD in the AP side was the same as in control Caco-2 cells (Fig. 6). Thus, the uptake

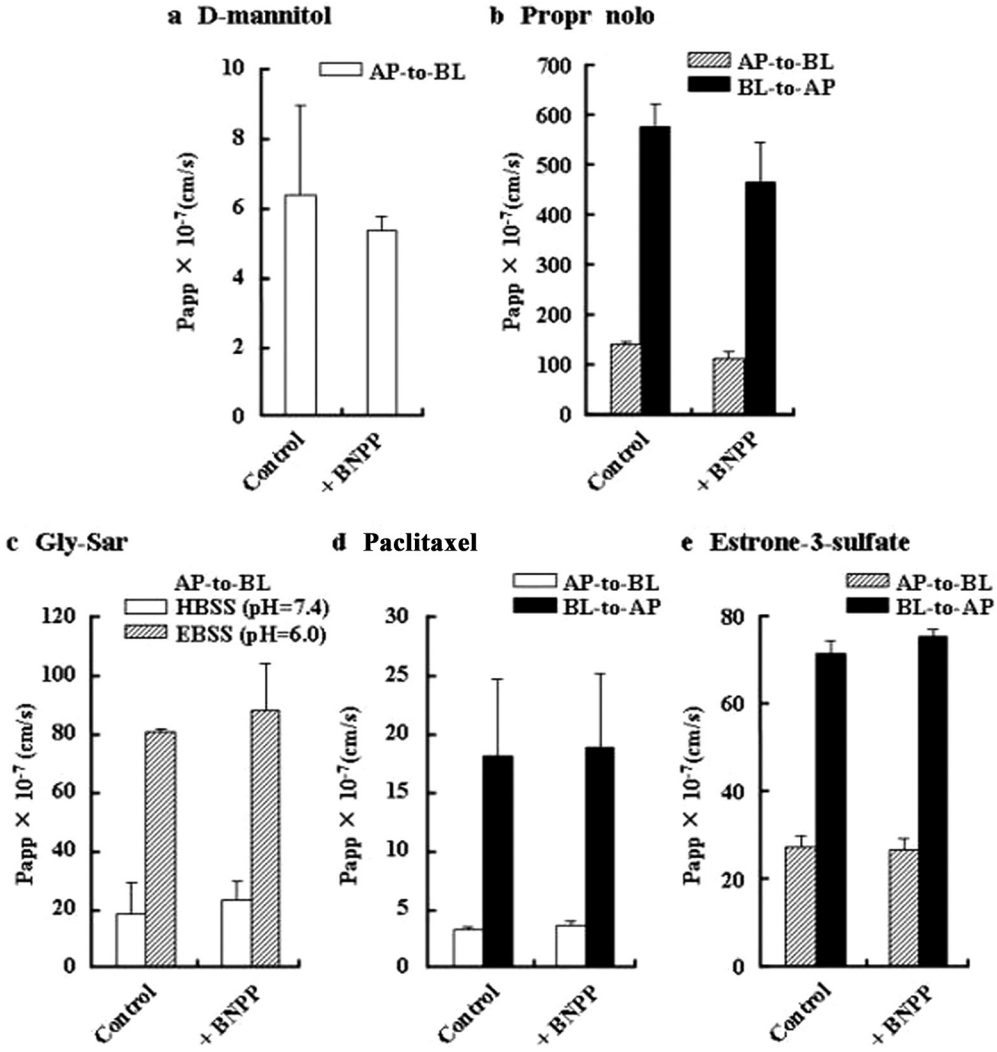

FIG. 4. Effect of BNPP on the transport of drugs via paracellular and transcellular routes across Caco-2 cell monolayers treated with BNPP at 200 μM. Control data are without BNPP treatment. a, AP-to-BL transport of [^{14}C]D-mannitol (1.2 μM) in HBSS (pH 7.4) on both sides. b, transport of propranolol (100 μM) in EBSS (pH 6.0) in the AP side and HBSS (pH 7.4) in the BL side. ▨, AP-to-BL transport; ■, BL-to-AP transport. c, AP-to-BL transport of [^{3}H]Gly-Sar (1 nM) in HBSS (pH 7.4, □) and in EBSS (pH 6.0, ▨) in the AP side and HBSS (pH 7.4) in the BL side. d, transport of [^{3}H]paclitaxel (2 nM) in HBSS (pH 7.4) in both sides. □, AP-to-BL transport; ■, BL-to-AP transport. e, transport of [^{3}H]estrone-3-sulfate (4 nM) in EBSS (pH 6.0) in the AP side and HBSS (pH 7.4) in the BL side. ▨, AP-to-BL transport; ■, BL-to-AP transport. Each column represent the mean ± S.D. (n = 3).

of ethyl-FXD from the AP compartment was not affected by BNPP, suggesting that BNPP treatment did not affect passive diffusion on the Caco-2 cellular membranes. In contrast to control Caco-2 cells, ethyl-FXD was mainly transported intact after treatment with BNPP. The P_{app} values for the transport of ethyl-FXD in the AP-to-BL direction after treatment with 200 μM BNPP was approximately 13 times higher than that of FXD (Table 2). The efflux ratio of permeability (BL-to-AP/AP-to-BL) was 1.20, indicating passive diffusion of ethyl-FXD. In the CES-inhibited condition, ethyl-FXD was poorly hydrolyzed to FXD, and FXD was only slowly transported into the BL compartment, as indicated by the extremely low cellular accumulation of FXD. Approximately 94% inhibition for the hydrolysis of ethyl-FXD under the treatment with BNPP was calculated by the total FXD amount converted from ethyl-FXD during the transport experiment for 2 h. Thus, it is predicted that ethyl-FXD is a prodrug well absorbed in its intact ester form by passive diffusion in the human small intestine.

Discussion

Caco-2 cells are widely used to evaluate drug absorption in the process of drug development. However, the expression levels of enzymes and transporters in Caco-2 cells show great variation, depending on the length of the culture period (Sun et al., 2002; Seithel et al., 2006). In the present study, we therefore investigated changes in the expression levels of CESs in Caco-2 cells after different culture periods. As shown in Fig. 1, both mRNA and protein levels of hCE1 and hCE2 were increased in a time-dependent manner, and hCE1 was always more highly expressed than hCE2. Sun et al. (2002) also reported the time-dependent mRNA expression of hCE1 and hCE2 and far higher expression of hCE1 than hCE2 in Caco-2 cells cultured until 16 days, according to GeneChip analysis.

Most commercially available prodrugs such as angiotensin-converting enzyme inhibitors, oseltamivir, and capecitabine, show high affinity for hCE1 but low affinity for hCE2 (Tabata et al., 2004; Imai, 2006; Shi et al., 2006). Therefore, the use of Caco-2 cells in screening may inaccurately predict the intestinal absorption of ester-type prodrugs because of their high expression of hCE1, especially in the case of parent drugs recognized by an efflux transporter on the brush-border membrane of Caco-2 cells. For example, in a transport experiment across Caco-2 cell monolayers, ME3229, an ester-type prodrug of a glycoprotein IIb/IIIa receptor antagonist, failed to show improved oral absorption due to transporter-mediated efflux of its hydrolyzed metabolites formed in Caco-2 cells (Okudaira et al., 2000).

Hence, we attempted to develop a novel evaluation system using Caco-2 cell monolayers to predict the absorption of prodrug in the absence of hCE1-mediated hydrolysis. However, a hCE1-specific inhibitor has not been developed until now, in contrast to the development of several specific hCE2 inhibitors such as loperamide,

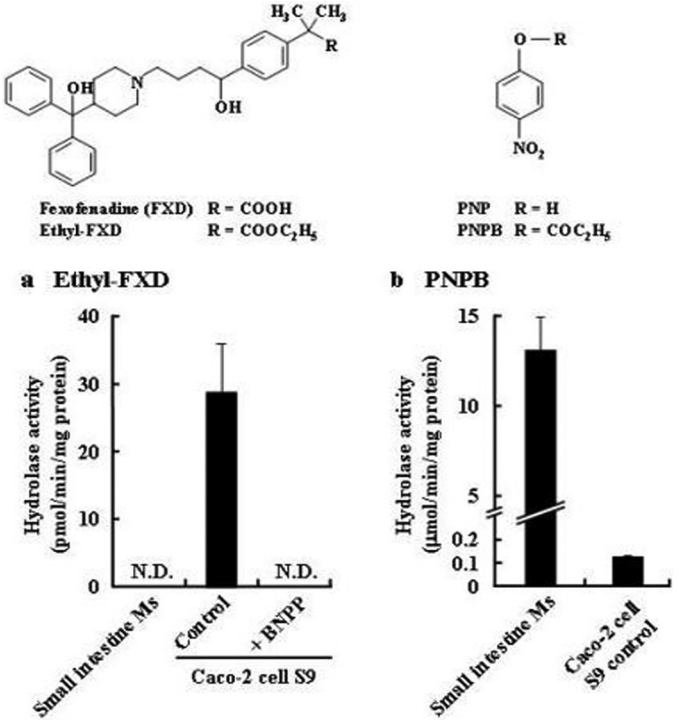

FIG. 5. Structure of ethyl-FXD and PNPB and hydrolysis of ethyl-FXD in Caco-2 cells treated with BNPP. a, hydrolysis of ethyl-FXD (30 μM) in human small intestinal microsomes and Caco-2 cell S9 prepared from cell monolayers treated with HBSS (control) or 200 μM BNPP. The microsomes and Caco-2 cell S9 were diluted with 50 mM HEPES buffer (pH 7.4) at 100 and 400 μg/ml, respectively. N.D., FXD was not detected. b, hydrolysis of PNPB (500 μM) in human small intestinal microsomes and Caco-2 cell S9. The microsomes and Caco-2 cell S9 were diluted with 50 mM HEPES buffer (pH 7.4) at 5 and 400 μg/ml, respectively. Each column represents the mean ± S.D. ($n = 3$).

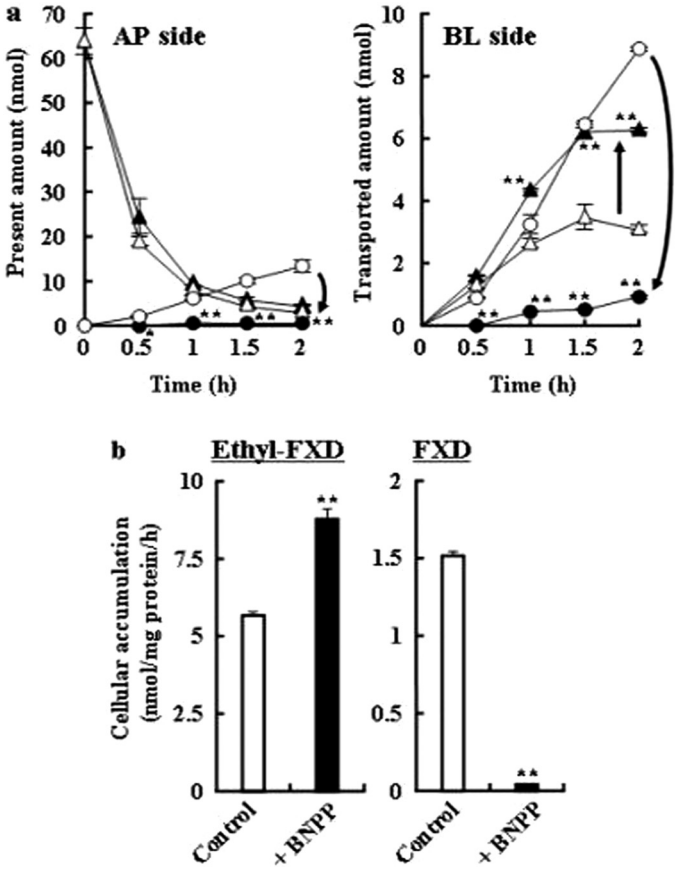

FIG. 6. The AP-to-BL transport of ethyl-FXD (40 μM) across Caco-2 cell monolayers with or without treatment with 200 μM BNPP (a) and cellular accumulation of ethyl-FXD and FXD (b). The transport experiments were performed in HBSS buffer (pH 7.4). Triangle and circle symbols represent the transport of ethyl-FXD and FXD, respectively. Open symbols and columns, transport across control Caco-2 cell monolayers; closed symbols and columns, transport through Caco-2 cell monolayers after treatment with BNPP. Each symbol and column represent the mean ± S.D. ($n = 3$). **, $p < 0.01$; *, $p < 0.05$, compared with control group.

benzyl, and 1-(2-chlorophenyl)-2-(3,4-dimethoxyphenyl)ethane-1,2-dione, a benzyl analog (Wadkins et al., 2005). First, we checked the inhibition effects of three CES inhibitors, diisopropyl phosphonate, PMSF, and BNPP, on the activities of dipeptidyl peptidase-IV and aminopeptidase in Caco-2 cell S9. Both diisopropyl phosphonate and PMSF inhibited their activities, but BNPP did not, even at a concentration of 1 mM (data not shown). We have demonstrated previously that pretreatment with 400 μM BNPP led to the inhibition of CES-mediated hydrolysis and a 3-fold increase in the absorption of *O*-isovaleryl-PL in rat jejunal single-pass perfusion, without altering aminopeptidase activity or the transport of L-leucyl-*p*-nitroanilide (Masaki et al., 2007). Furthermore, the hydrolase activities of both hCE1 and hCE2 for PNPB were inhibited by more than 90% at 10 μM BNPP and almost 100% at 50 μM BNPP, using the recombinant enzymes expressed in HEK293 cells (data not shown). Thus, BNPP inhibits both hCE1 and hCE2 but almost never other serine esterases. Based on these results, we selected BNPP as a specific inhibitor of CES. As shown in Table 1, the P_{app} for butyryl-PL and its hydrolysis percentage were constant after treatment with more than 200 μM BNPP. Moreover, cytotoxicity attributed to BNPP was not observed on treatment with up to 500 μM BNPP according to TEER values and staining by trypan blue. Consequently, we decided to pretreat with 200 μM BNPP for 40 min before the transport experiments.

When prodrugs permeate across Caco-2 cell monolayers, they are hydrolyzed by not only CESs but also esterases presented on the cellular membrane. The hydrolysis of butyryl-PL during transport across Caco-2 cell monolayers was 86% inhibited by BNPP, although it was almost completely inhibited in the cellular S9 fractions prepared after the treatment with 200 μM BNPP (Fig. 3). Therefore, CESs are responsible for 86% of hydrolysis of butyryl-PL in Caco-2 cell monolayers, and the remaining 14% of hydrolase activity may be accounted for by esterases present on Caco-2 cell membranes. Masaki et al. (2007) also reported that CESs accounted for approximately 85% of hydrolysis of *O*-isovaleryl-PL in rat jejunal single-pass perfusion. Our results are in agreement with previous studies, suggesting that the intestinal absorption of ester compounds can be predicted well using this transport experiment in Caco-2 cell monolayers treated with BNPP. In contrast, BNPP treatment inhibited 94% of the hydrolysis of ethyl-FXD during transport across Caco-2 cell monolayers for 2 h, indicating that hydrolysis of ethyl-FXD is attributed mainly to CES,

TABLE 2

P_{app} values for the AP-to-BL and BL-to-AP transport of FXD and ethyl-FXD through Caco-2 cell monolayers treated with BNPP

P_{app} values of ethyl-FXD were calculated from the total amount of ethyl-FXD and FXD in the receiver side after treatment with 200 μM BNPP. Values represent the mean ± S.D. ($n = 3$).

Compound	P_{app}		Ratio (BL-to-AP/AP-to-BL)
	AP-to-BL	BL-to-AP	
	$\times 10^{-7}$ cm/s		
FXD (44 μM)	5.24 ± 1.05	14.9 ± 0.840	2.85
Ethyl-FXD (40 μM)	75.4 ± 1.64	90.8 ± 6.73	1.20

and the contribution of membrane esterases is small. The inhibitory effect of BNPP varies for each substrate according to the extent of hydrolysis catalyzed by CES, which suggests that the hydrolytic conditions of Caco-2 cells treated with BNPP may be able to reflect the hydrolytic characteristics of the human small intestine.

The effect of BNPP on the permeability of different drugs via various transport pathways was also demonstrated. It has been reported that protease inhibitors, such as bacitracin, aprotinin, and BMS-262084 (Kamath et al., 2005), enhance the absorption of phenol red, fluorescein isothiocyanate dextrans, or inulin, suggesting opening of the tight junction (Gotoh et al., 1996; Machida et al., 2000). However, as shown in Fig. 4a, the permeability of D-mannitol, as a marker of paracellular diffusion, was not affected by the BNPP treatment. The TEER values were maintained at 1000 to 1200 $\Omega \cdot cm^2$ until the transport experiment was completed (data not shown). These results suggest that treatment with 200 μM BNPP causes no damage to tight junctions of Caco-2 cell monolayers. Furthermore, neither passive diffusion nor the function of transporters such as hPEPT1, P-gp, BCRP, and OATP2B1 was influenced by pretreatment with 200 μM BNPP. Thus, this evaluation system provides optimal conditions for paracellular and transcellular transport across Caco-2 cell monolayers. From the viewpoint of hydrolysis and membrane transport, this novel evaluation system, using Caco-2 cells under CES inhibition, has great potential in the assessment of intestinal transport of ester-type prodrugs.

Finally, we evaluated the utility of the system for predicting the intestinal absorption of ethyl-FXD as a model prodrug that improves poor intestinal absorption of FXD. As shown in Fig. 5, ethyl-FXD is well hydrolyzed in Caco-2 cells, being a good substrate for hCE1 and a poor one for hCE2. When we performed the AP-to-BL transport experiment of ethyl-FXD in Caco-2 cell monolayers, ethyl-FXD was extensively hydrolyzed to FXD, and FXD was dominantly transported in both AP and BL side (Fig. 6). However, ethyl-FXD is marginally hydrolyzed in human small intestinal microsomes. Therefore, the ability to evaluate accurately the intestinal absorption of ethyl-FXD in normal Caco-2 cell monolayers was impeded. In contrast, Caco-2 cell monolayers treated with BNPP inhibited 94% of the hydrolysis of ethyl-FXD, followed by a significant decrease in the cellular accumulation and transport of FXD. Therefore, the permeation of ethyl-FXD across Caco-2 cell monolayers under CES-inhibited conditions could predict its intestinal absorption in humans. Ethyl-FXD was rapidly taken up and accumulated into Caco-2 cells. When the P_{app} value was calculated by the transported amount of ethyl-FXD in the receiver side, it was $67.4 \pm 1.81 \times 10^{-7}$ cm/s. This value indicates high absorption, judging from the correlation between the absorbed fraction in humans after oral administration and the permeability in Caco-2 cell monolayers (Grès et al., 1998; Artursson et al., 2001). In addition, there was no significant difference in the P_{app} values of ethyl-FXD between the AP-to-BL and BL-to-AP transport after treatment with BNPP (Table 2). This result suggests that the intestinal transport of ethyl-FXD is not affected by efflux via P-gp. Therefore, it is predicted that ethyl-FXD is absorbed in an intact form by passive diffusion in human small intestine and shows high oral absorption. It is interesting that the recognition of FXD by P-gp was altered by chemical modification of its carboxylic acid.

We have been unable to elucidate why hCE1 is significantly upregulated and the expression of hCE2 is unusually low in Caco-2 cells, but low hCE2 levels may be ascribable to some transcriptional and epigenetic regulations. There is a report that p53, a tumor suppressor, directly bound to the first intron of the hCE2 gene, induces hCE2 expression, but hCE2 is not induced in p53-null cells or cells expressing mutated p53 (Choi et al., 2006). Because Caco-2 cells have been shown to have mutant p53 (Gartel et al., 2003), this mutation may down-regulate hCE2 in Caco-2 cells. DNA hypermethylation may also be a mechanism contributing to the down-regulation of hCE2, because several GC boxes exist in the promoter region of hCE2 gene (Wu et al., 2003).

Despite the clear difference in the expression of CES between human small intestine and Caco-2 cells, the latter have been the most popular model for permeability assays in drug discovery over the last two decades. Therefore, it is suggested that the novel in vitro evaluation system using CES-inhibited Caco-2 cell monolayers described in this study may be extremely effective for the prediction of human intestinal absorption of ester-type prodrugs, which are scarcely hydrolyzed by hCE2. It is unfortunate that this system is not appropriate for evaluation of the permeability of compounds hydrolyzed by only hCE2. For the prediction of permeability of hCE2 substrates, the desire is to develop Caco-2 cells that show high-level expression of hCE2 and low-level expression of hCE1.

References

Artursson P, Palm K, and Luthman K (2001) Caco-2 monolayers in experimental and theoretical predictions of drug transport. *Adv Drug Deliv Rev* **46:**27–43.

Block W and Arndt R (1978) Chromatographic study on the specificity of bis-p-nitrophenylphosphate in vivo. Identification of labelled proteins of rat liver after intravenous injection of bis-*p*-nitro[^{14}C]phenylphosphate as carboxylesterases and amidases. *Biochim Biophys Acta* **524:**85–93.

Borlak J and Zwadlo C (2003) Expression of drug-metabolizing enzymes, nuclear transcription factors and ABC transporters in Caco-2 cells. *Xenobiotica* **33:**927–943.

Bradford MM (1976) A rapid and sensitive method for the quantitation of microgram quantities of protein utilizing the principle of protein-dye binding. *Anal Biochem* **72:**248–254.

Choi W, Cogdell D, Feng Y, Hamilton SR, and Zhang W (2006) Transcriptional activation of the carboxylesterase 2 gene by the p53 pathway. *Cancer Biol Ther* **5:**1450–1456.

Di Giacomo B, Coletta D, Natalini B, Ni MH, and Pellicciari R (1999) A new synthesis of carboxyterfenadine (fexofenadine) and its bioisosteric tetrazole analogs. *Farmaco* **54:**600–610.

Gartel AL, Feliciano C, and Tyner AL (2003) A new method for determining the status of p53 in tumor cell lines of different origin. *Oncol Res* **13:**405–408.

Gotoh S, Nakamura R, Nishiyama M, Quan YS, Fujita T, Yamamoto A, and Muranishi S (1996) Effects of protease inhibitors on the absorption of phenol red and fluorescein isothiocyanate dextrans from the rat intestine. *J Pharm Sci* **85:**858–862.

Gram LK, Rist GM, Lennernäs H, and Steffansen B (2009) Impact of carriers in oral absorption: permeation across Caco-2 cells for the organic anions estrone-3-sulfate and glipizide. *Eur J Pharm Sci* **37:**378–386.

Grès MC, Julian B, Bourrié M, Meunier V, Roques C, Berger M, Boulenc X, Berger Y, and Fabre G (1998) Correlation between oral drug absorption in humans, and apparent drug permeability in TC-7 cells, a human epithelial intestinal cell line: comparison with the parental Caco-2 cell line. *Pharm Res* **15:**726–733.

Heymann E and Krisch K (1967) Phosphoric acid-bis-(*p*-nitro-phenylester), a new inhibitor of microsomal carboxylesterases. *Hoppe Seylers Z Physiol Chem* **348:**609–619.

Hidalgo IJ and Li J (1996) Carrier-mediated transport and efflux mechanisms in Caco-2 cells. *Adv Drug Deliv Rev* **22:**53–66.

Imai T (2006) Human carboxylesterase isozymes: catalytic properties and rational drug design. *Drug Metab Pharmacokinet* **21:**173–185.

Imai T, Imoto M, Sakamoto H, and Hashimoto M (2005) Identification of esterases expressed in Caco-2 cells and effects of their hydrolyzing activity in predicting human intestinal absorption. *Drug Metab Dispos* **33:**1185–1190.

Jeong EJ, Liu Y, Lin H, and Hu M (2005) Species- and disposition model-dependent metabolism of raloxifene in gut and liver: role of UGT1A10. *Drug Metab Dispos* **33:**785–794.

Kamath AV, Morrison RA, Harper TW, Lan SJ, Marino AM, and Chong S (2005) Multiple pathways are involved in the oral absorption of BMS-262084, a tryptase inhibitor, in rats: role of paracellular transport, binding to trypsin, and P-glycoprotein efflux. *J Pharm Sci* **94:**1115–1123.

Machida M, Hayashi M, and Awazu S (2000) The effects of absorption enhancers on the pulmonary absorption of recombinant human granulocyte colony-stimulating factor (rhG-CSF) in rats. *Biol Pharm Bull* **23:**84–86.

Masaki K, Hashimoto M, and Imai T (2007) Intestinal first-pass metabolism via carboxylesterase in rat jejunum and ileum. *Drug Metab Dispos* **35:**1089–1095.

Masaki K, Taketani M, and Imai T (2006) First-pass hydrolysis of a propranolol ester derivative in rat small intestine. *Drug Metab Dispos* **34:**398–404.

Mentlein R, Rix-Matzen H, and Heymann E (1988) Subcellular localization of non-specific carboxylesterases, acylcarnitine hydrolase, monoacylglycerol lipase and palmitoyl-CoA hydrolase in rat liver. *Biochim Biophys Acta* **964:**319–328.

Nakamura T, Sakaeda T, Ohmoto N, Tamura T, Aoyama N, Shirakawa T, Kamigaki T, Nakamura T, Kim KI, Kim SR, et al. (2002) Real-time quantitative polymerase chain reaction for MDR1, MRP1, MRP2, and CYP3A-mRNA levels in Caco-2 cell lines, human duodenal enterocytes, normal colorectal tissues, and colorectal adenocarcinomas. *Drug Metab Dispos* **30:**4–6.

Nishimura M, Yoshitsugu H, Naito S, and Hiraoka I (2002) Evaluation of gene induction of drug-metabolizing enzymes and transporters in primary culture of human hepatocytes using high-sensitivity real-time reverse transcription PCR. *Yakugaku Zasshi* **122:**339–361.

Okudaira N, Komiya I, and Sugiyama Y (2000) Polarized efflux of mono- and diacid metabolites of ME3229, an ester-type prodrug of a glycoprotein IIb/IIIa receptor antagonist, in rat small intestine. *J Pharmacol Exp Ther* **295:**717–723.

Perloff MD, von Moltke LL, and Greenblatt DJ (2002) Fexofenadine transport in Caco-2 cells: inhibition with verapamil and ritonavir. *J Clin Pharmacol* **42:**1269–1274.
Pinto M, Robine-Leon S, Appay MD, Kedinger M, Triadou N, Dussaulx E, Lacroix B, Simmon-Assmann P, Haffen K, Fogh J, et al. (1983) Enterocyte-like differentiation and polarization of the human colon carcinoma cell line Caco-2 in culture. *Biol Cell* **47:**323–330.
Raeissi SD, Hidalgo IJ, Segura-Aguilar J, and Artursson P (1999) Interplay between CYP3A-mediated metabolism and polarized efflux of terfenadine and its metabolites in intestinal epithelial Caco-2 (TC7) cell monolayers. *Pharm Res* **16:**625–632.
Satoh T, Taylor P, Bosron WF, Sanghani SP, Hosokawa M, and La Du BN (2002) Current progress on esterases: from molecular structure to function. *Drug Metab Dispos* **30:**488–493.
Seithel A, Karlsson J, Hilgendorf C, Björquist A, and Ungell AL (2006) Variability in mRNA expression of ABC- and SLC-transporters in human intestinal cells: comparison between human segments and Caco-2 cells. *Eur J Pharm Sci* **28:**291–299.
Shameem M, Imai T, and Otagiri M (1993) An in-vitro and in-vivo correlative approach to the evaluation of ester prodrugs to improve oral delivery of propranolol. *J Pharm Pharmacol* **45:**246–252.
Shi D, Yang J, Yang D, LeCluyse EL, Black C, You L, Akhlaghi F, and Yan B (2006) Anti-influenza prodrug oseltamivir is activated by carboxylesterase human carboxylesterase 1, and the activation is inhibited by antiplatelet agent clopidogrel. *J Pharmacol Exp Ther* **319:**1477–1484.
Siissalo S, Zhang H, Stilgenbauer E, Kaukonen AM, Hirvonen J, and Finel M (2008) The expression of most UDP-glucuronosyltransferases (UGTs) is increased significantly during Caco-2 cell differentiation, whereas UGT1A6 is highly expressed also in undifferentiated cells. *Drug Metab Dispos* **36:**2331–2336.
Sun D, Lennernas H, Welage LS, Barnett JL, Landowski CP, Foster D, Fleisher D, Lee KD, and Amidon GL (2002) Comparison of human duodenum and Caco-2 gene expression profiles for 12,000 gene sequences tags and correlation with permeability of 26 drugs. *Pharm Res* **19:**1400–1416.
Tabata T, Katoh M, Tokudome S, Nakajima M, and Yokoi T (2004) Identification of the cytosolic carboxylesterase catalyzing the 5′-deoxy-5-fluorocytidine formation from capecitabine in human liver. *Drug Metab Dispos* **32:**1103–1110.
Takai S, Matsuda A, Usami Y, Adachi T, Sugiyama T, Katagiri Y, Tatematsu M, and Hirano K (1997) Hydrolytic profile for ester- or amide-linkage by carboxylesterases pI 5.3 and 4.5 from human liver. *Biol Pharm Bull* **20:**869–873.
Tang M, Mukundan M, Yang J, Charpentier N, LeCluyse EL, Black C, Yang D, Shi D, and Yan B (2006) Antiplatelet agents aspirin and clopidogrel are hydrolyzed by distinct carboxylesterases, and clopidogrel is transesterificated in the presence of ethyl alcohol. *J Pharmacol Exp Ther* **319:**1467–1476.
Tsuji A and Tamai I (1996) Carrier-mediated intestinal transport of drugs. *Pharm Res* **13:**963–977.
Wadkins RM, Hyatt JL, Wei X, Yoon KJ, Wierdl M, Edwards CC, Morton CL, Obenauer JC, Damodaran K, Beroza P, et al. (2005) Identification and characterization of novel benzil (diphenylethane-1,2-dione) analogues as inhibitors of mammalian carboxylesterases. *J Med Chem* **48:**2906–2915.
Watkins PB (1997) The barrier function of CYP3A4 and P-glycoprotein in the small bowel. *Adv Drug Deliv Rev* **27:**161–170.
Wu MH, Chen P, Remo BF, Cook EH Jr, Das S, and Dolan ME (2003) Characterization of multiple promoters in the human carboxylesterase 2 gene. *Pharmacogenetics* **13:**425–435.
Yamashita S, Tanaka Y, Endoh Y, Taki Y, Sakane T, Nadai T, and Sezaki H (1997) Analysis of drug permeation across Caco-2 monolayer: implication for predicting in vivo drug absorption. *Pharm Res* **14:**486–491.

Address correspondence to: Dr. Teruko Imai, Professor, Graduate School of Pharmaceutical Sciences, Kumamoto University, 5-1 Oe-Honmachi, Kumamoto 862-0973, Japan. E-mail: iteruko@gpo.kumamoto-u.ac.jp